8. Phosphorus, Barium, Manganese, and Uranium Concentrations and Geochemistry, Nazca Ridge Site 1237 Sediments[1]

Cecily O.J. Chun[2] and Margaret L. Delaney[2]

ABSTRACT

We determined the sedimentary concentrations of phosphorus (P), barium (Ba), manganese (Mn), titanium (Ti), aluminum (Al), and uranium (U) for sediment samples from the southeast Pacific Nazca Ridge, Ocean Drilling Program Site 1237. This unique record extends to 31 Ma over 360 meters composite depth (mcd), recording depositional history as the site progressed eastward over its paleohistory. We sampled with a temporal resolution of ~0.2 m.y. throughout the sequence, equivalent to an average spacing of 1.63 m/sample. Concentrations of sequentially extracted components of P (oxide-associated, authigenic, organic, and detrital) increase toward the modern. Al/Ti ratios indicate that the background detrital source material is consistent with upper continental crust. U enrichment factors (U_{EFs}) generally exceed crustal values and indicate slightly reducing environments. However, authigenic U precipitation can also be influenced by the organic carbon rain rate and may not be solely an indicator of redox conditions. Dramatic changes in Mn_{EFs} at ~162 mcd, from values between 12 and 93 to values <12 after this depth, and a sharp color contact boundary lead us to believe that a paleoredox boundary from an oxygenated to a more reducing depositional environment occurred near this depth. Estimates of biogenic barite concentrations from a total sediment digestion technique (Ba_{excess}) are greater than those from a barite extraction (Ba_{barite}) for selected samples across the entire depth range. Applying a range of Ba/Ti ratios from different source materials to correct for detrital inputs does not change

the lack of agreement with Ba_{barite} concentrations. Reactive P ($P_{reactive}$) concentrations (the sum of oxide-associated, authigenic, and organic P concentrations) increase toward the modern with values typically <12 µmol P/g from the base of our record through ~100 mcd, with a gradual increase to concentrations >15 µmol P/g. Ba_{excess} follows the same general trends as $P_{reactive}$, with concentrations <14 µmol Ba/g in the lower portion of the record to values >15 µmol Ba/g. Accumulation rate records of these proxies will be needed to infer paleoproductivity. $P_{reactive}$/Ba_{excess} ratios, an indicator of the relative burial of the nutrient P to organic carbon export, exhibit higher values, similar to modern, from the base of our record through ~180 mcd. The remainder of the record exhibits values lower than modern, indicating that organic carbon export to the sediments was higher relative to nutrient burial.

INTRODUCTION

Ocean Drilling Program (ODP) Leg 202 recovered the longest continuous sediment sequence ever collected from the southeast Pacific at Nazca Ridge Site 1237 (modern water depth = ~3212 m), extending from the late Oligocene through the Holocene. Because Nazca Ridge is a fossil hotspot, its paleoceanographic position can be backtracked. Site 1237 is estimated to have migrated ~20° eastward toward South America over the past 30 m.y. (Mix, Tiedemann, Blum, et al., 2003). Modern regional changes in surface nutrients and productivity as this site moved from the open-ocean site to the coast predict a dramatic increase in productivity. Major tectonic events have also influenced the environments of the southeast Pacific. Andean uplift, which occurred in the last 10 m.y., forms a barrier for atmospheric circulation in the South Pacific by forcing low-level high-velocity winds along the coast line. This results in enhanced coastal upwelling, another forcing factor for potential increased productivity.

The sediment characteristics of Site 1237 were described on board the ship and divided into two major lithologic units, Units I and II, divided at 100 meters composite depth (mcd). Unit I has a greater proportion of siliceous microfossils (>75 wt% at 5 and 40 mcd) and fewer calcareous microfossils ($CaCO_3$ wt% ≤ 50%) than Unit II and a greater proportion of siliciclastics in the upper 30 mcd, based on shipboard smear slide samples. There are distinct layers of Andean ash in Unit I. These findings are consistent with the paleobacktracking of Nazca Ridge as it moved closer to the productive upwelling centers near South America. In addition, sediment color changes abruptly at ~162 mcd, from fairly homogeneous pale brown (in sediments below ~162 mcd) to a grayish white, without being associated with any major lithologic change (Mix, Tiedemann, Blum, et al., 2003). Shipboard interstitial water measurements of manganese (Mn) and sulfate (SO_4^{2-}) indicate no sulfate reduction or major present-day redox changes at this depth (Mix, Tiedemann, Blum, et al., 2003).

Our study uses multiple sedimentary geochemical proxies, including reactive phosphorus ($P_{reactive}$), Al/Ti molar ratios, the enrichment factors (EFs) of Mn and U, and excess Ba. $P_{reactive}$ and excess Ba are tracers of nutrient burial and paleoproductivity. Al/Ti molar ratios are used to characterize terrigenous source material rocks. The redox-sensitive trace metals Mn and U describe the redox conditions during sediment burial. We examine if a change in paleoredox conditions or source supply in-

fluenced the dramatic color change at ~162 mcd. Ultimately, with a refined age model that will allow us to take the concentrations of our proxies into accumulation rates, we will be able to characterize the history of nutrient burial and paleoredox conditions at Site 1237.

Phosphorus is the ultimate limiting nutrient to oceanic primary production on geologic timescales (Tyrrell, 1999). P is delivered to the sediment-water interface primarily as organic P. Transformations of organic and oxide-associated P to authigenic P in marine sediments at continental margins and open-ocean sites occurs during sediment burial (e.g., Ruttenberg and Berner, 1993; Filippelli and Delaney, 1996; Anderson et al., 2001). Therefore, using total reactive P ($P_{reactive}$, defined as the sum of organic, oxide-associated, and authigenic P) more accurately describes the geochemical behavior of sedimentary P rather than using organic P or bulk total P alone. Our study uses the modified sequential extraction procedure of Anderson and Delaney (2000) to quantify the components of P and to separate the bioavailable P, reported as $P_{reactive}$, from detrital P.

Another key piece of information to accurately describe paleoenvironments and to validate the use of other proxies is the sedimentary redox state at or near the time of deposition. Redox-sensitive metal EFs relative to crustal averages help describe the depositional environments of the sediments at the time of burial. Al/Ti ratios allow us to identify source rock characteristics which are needed to calculate EFs. Authigenic U enrichments in marine sediments occur in both suboxic to anoxic surface sediments and subsurface suboxic to anoxic deposits underlying bottom water oxic conditions. Furthermore, it has been demonstrated that the export of organic carbon from the overlying water column can also influence authigenic U precipitation (Calvert and Pedersen, 1993; Rosenthal et al., 1995; Chase et al., 2001; McManus et al., 2005). Because of the multiple sources for authigenic U formation, we use the approach that the absence of U enrichment suggests sedimentation under oxygenated bottom water conditions.

When dissolved Mn in sediment interstitial waters diffuses upward into overlying oxic near-surface interstitial or bottom waters, it reprecipitates, forming Mn oxyhydroxides. Authigenic Mn enrichment in marine sediments is one of the most reliable indicators of oxic bottom water conditions because the source of excess dissolved Mn in interstitial waters occurs only where the sediment-water interface accumulates Mn oxyhydroxides. These areas occur only beneath oxygenated bottom waters (Calvert and Pedersen, 1993); therefore, Mn enrichment (EF > 1) strongly indicates oxygenated bottom waters at time of sediment burial.

Biogenic barite ($BaSO_4$) found in marine environments is closely associated with decaying organic matter (Dehairs et al., 1980; Bishop, 1988; Ganeshram et al., 2003). The positive correlations between barite associated with organic matter, biogenic barite, and organic carbon fluxes as measured in sediment trap studies (Dymond et al., 1992; Dymond and Collier, 1996; Eagle et al., 2003) suggest that the accumulation of biogenic barite, generally a more refractive chemical species than organic carbon, can be used as a paleoproductivity proxy of carbon export in the oceans (Dymond, et al., 1992; Paytan and Kastner, 1996; Paytan et al., 1996). Two approaches for quantifying biogenic barite in marine sediments are used in this study: (1) measuring the total Ba concentration and correcting for detrital inputs, defined here as Ba_{excess} used in all samples, and (2) barite separated from sediments according to a sequential extraction technique (Paytan and Kastner, 1996;

Paytan et al., 1996; Eagle et al., 2003), defined here as Ba_{barite} used in a small number of samples. We will compare the results of both approaches and evaluate their strengths and weaknesses.

$P_{reactive}/Ba_{excess}$ ratios, when compared to predicted values, have been proposed to be indicators of the efficiency of nutrient burial at the sediment-water interface relative to export of organic matter buried in the sediments (Nilsen et al., 2003). We will compare our results to the expected $P_{reactive}/Ba_{excess}$ ratios for the modern Atlantic and Pacific, 2–13, as predicted from Dymond et al. (1992), Anderson and Sarmiento (1994), and François et al. (1995).

METHODS

This study uses sediments collected from Site 1237. Our sample resolution is ~0.2 m.y., using the smoothed linear sedimentation rate age model calculated on board the ship (Mix, Tiedemann, Blum, et al., 2003), throughout the 31-m.y. record. This averages approximately one sample every 1.63 m. All samples were treated uniformly: freeze-dried, crushed, and sieved with a 150-µm mesh. P concentrations of marine sediments were measured on 100-mg samples following treatment with a four-step extraction (as modified by Anderson and Delaney [2000], after Ruttenberg [1992]). Quantifiable components of $P_{reactive}$ are operationally defined as oxide-associated P, authigenic P, and organic P. This analytical procedure also identifies detrital P, which is not biologically available in the water column. P concentrations were measured directly from the extractants by a LaChat Quick Chem 8000 automated spectrophotometric flow injection analysis system (Anderson and Delaney, 2000). Detection limits and reproducibility of a consistency standard are reported in Table T1.

Ba, Mn, U, Ti, and Al concentrations were measured according to a total sediment acid digestion method (Environmental Protection Agency [EPA] SW-836 Method 3052) on 50-mg samples. Samples were digested with 5 mL of concentrated nitric acid (16 N) and 1 mL of concentrated hydrofluoric acid (28.9 N) overnight in Teflon bombs. They were then microwaved at 12% power for 90 min and taken to dryness on a hotplate. Acids (1 mL each of 16-N HNO_3, 12-N HCl, and 16-N HNO_3) were sequentially added, with drying on the hotplate between each addition. Samples were then redissolved in 1 mL of 16-N HNO_3, 0.5 mL of 30% H_2O_2, 0.1 mL of 28.9-N HF, and 5 mL of glass-distilled water. Analyses for Mn, U, and Ti were performed using a Finnigan Element high-resolution inductively coupled plasma (ICP)–mass spectrometer. Al and Ba were measured on a PerkinElmer Optima 4300 DV ICP–optical emission spectrometer. Detection limits and reproducibility of a consistency standard are reported in Table T1. Al/Ti molar ratios were plotted and compared to published values: 38 for upper crust, 34 for middle crust, 32 for lower crust, and 35 for bulk (total) crust (Rudnick and Gao, 2004). Trace metal EFs for Mn and U were calculated as EF = $(metal/Ti)_{sample}/(metal/Ti)_{crust}$, using the upper crustal ratios Mn/Ti (mol/mol) = 0.176 and U/Ti (mmol/mol) = 0.142 (Rudnick and Gao, 2004).

Ba_{excess}, representing biogenic barite, was determined by measuring total Ba and correcting for detrital input and is defined here as

$$Ba_{excess} = Ba_{(total)} - [Ti \times (Ba/Ti)_{crust}].$$

In this study, we used the upper crustal molar ratio of Ba/Ti = 0.057 (Rudnick and Gao, 2004). In order to evaluate the error associated with choosing bulk crustal elemental ratios for our normalization calculations, we also calculated Ba_{excess} for selected samples with a range of Ba/Ti ratios from the published literature, with all ratios in molar units:

Ba/Ti = 0.009 for carbonates (Turekian and Wedepohl, 1961),
Ba/Ti = 0.037 for bulk crustal (Rudnick and Gao, 2004),
Ba/Ti = 0.043 for Ca-rich granites (Turekian and Wedepohl, 1961),
Ba/Ti = 0.057 for the upper crust (Rudnick and Gao, 2004), and
Ba/Ti = 0.174 for deep-sea clays (Turekian and Wedepohl, 1961).

Barite separated from sediments according to a sequential leaching procedure (Paytan et al., 1996; Eagle et al., 2003) is defined here as Ba_{barite}. Measurements of Ba_{barite} on selected samples were performed by Paytan at her laboratory at Stanford University, California (USA) and are reported in Ba micromoles per gram calculated from the weight percent barite extracted:

$$\mu mol\ Ba/g\ sediment = [(weight\%\ barite\ extracted/100)/molar\ weight\ of\ barite] \times 10^6.$$

RESULTS

Authigenic P, which is the dominant form of P in marine sediments, exhibits concentrations <12 µmol P/g throughout Unit II with values increasing from the base of Unit I to maximum concentrations of 21 µmol P/g at 15.34 mcd (Fig. F1; Table T2). Organic and oxide-associated P concentrations are low in Unit II with values <2 µmol P/g and oxide-associated P below detection limit in most of our samples (Fig. F1; Table T2). In Unit I, organic P displays highest concentrations at 21.70 mcd with a value of 4.58 µmol P/g, whereas oxide-bound P displays the highest concentration of 1.56 µmol P/g at 3.44 mcd. Detrital P values are generally <1 µmol P/g throughout most of Unit II with increasing values in Unit I, peaking at 21.70 mcd with a value of 9.33 µmol P/g.

Al and Ti concentrations are correlated in these samples (Fig. F2), indicating a consistent dominant detrital source material. The Al/Ti ratio of this data set slope of regression line is 38.8 ± 0.4 mol/mol (mean Al/Ti of all samples is 47.4 ± 18.7 mol/mol) and is consistent with using an upper crust source rock ratio (38 mol/mol; Rudnick and Gao, 2004). Therefore, it is appropriate to use elemental ratios of upper crust throughout our record, for all of our normalization calculations (U_{EF}, Mn_{EF}, and Ba_{excess}). U_{EFs} are generally >1 throughout the sedimentary record and range between 0.83 and 7.4 (Fig. F3A; Table T2). Mn_{EFs} are generally >15 and as much as 93 below the color change boundary and decrease to values <10 and as little as 0.63 above ~162 mcd (Fig. F3B; Table T2).

Selected samples separated for Ba_{barite} have values ranging between 10.7 µmol Ba/g at 10.8 mcd and 0.16 µmol Ba/g at 266.91 mcd (Table T3). The sequential leaching technique to separate biogenic barite crystals confirmed the presence of unaltered marine barite crystals in tested samples. Ba_{excess} concentrations are consistently higher than Ba_{barite} measurements for the same samples (Fig. F4; Table T3). Calculations of Ba_{excess} using a range of published Ba/Ti ratios for source materials exhibit
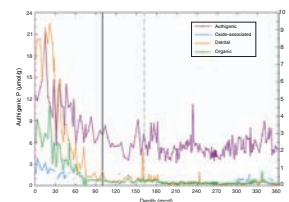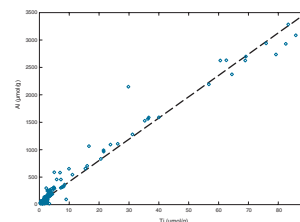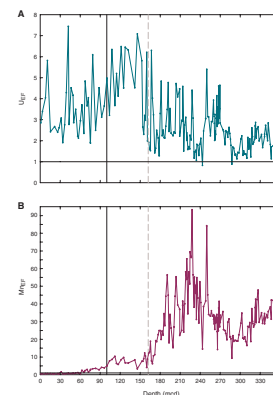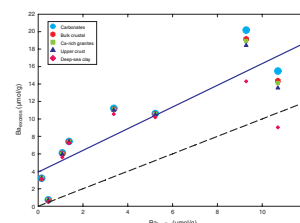
the greatest variability for those samples containing higher detrital concentrations, Ba_{barite} >6 µmol Ba/g and <60% $CaCO_3$ wt%, as expected (Fig. F4; Table T3). Regardless of source material Ba/Ti ratio used in normalization, Ba_{excess} is greater than Ba_{barite}, falling above a 1:1 line, with the exception of the most detrital-rich sample using the deep-sea clay normalization (Fig. F4). The comparison of Ba_{excess} and Ba_{barite} did not change when we used Ba/Al for normalization (not shown). Because using different Ba/Ti ratios does not greatly change the overall trends in our data and our Al/Ti molar ratios are most similar to upper crustal values, we chose to apply the upper crustal Ba/Ti = 0.057 ratio (Rudnick and Gao, 2004) in our Ba_{excess} calculations for the downcore records.

Concentrations of $P_{reactive}$ are <12 µmol P/g in Unit II and gradually increase from the base of Unit I to >6 µmol P/g and a maximum of 25.3 µmol P/g at 15.34 mcd (Fig. F5A; Table T2). Ba_{excess} concentrations calculated relative to an upper crustal source are <14 µmol Ba/g in Unit II and increase at the transition to Unit I to peak values of 21.24 µmol Ba/g at 36.90 mcd (Fig. F5A; Table T2). Starting at ~270 mcd, $P_{reactive}$ and Ba_{excess} concentrations follow the same general trends through the upper remaining portion of Unit II and all of Unit I. $P_{reactive}/Ba_{excess}$ ratios have the highest values between ~360 and 300 mcd, between ~2 and 16 (Fig. F5B; Table T2). There is some variability between 220 and 180 mcd with ratios >2. The remainder of Unit II and all of Unit I exhibit $P_{reactive}/Ba_{excess}$ ratios <2.

DISCUSSION

Our geochemical observations of sedimentary P show that the average fraction of total reactive P that is authigenic, 95% ± 2%, agrees well with other published marine sediment P records (e.g., Filippelli and Delaney, 1995, 1996; Delaney and Anderson, 1997, 2000; Faul and Delaney, 2000; Anderson, et al., 2001; Faul et al., 2003; Nilsen et al., 2003). In our samples, the remaining components of total reactive sedimentary P on average, over the entire record, are much lower because the sediments are diagenetically more mature with 1% ± 2% in oxide-associated P and 4% ± 0.3% in organic P (Fig. F1; Table T2). The fraction of total P composed of organic and oxide-associated P is <10% in Unit II and highest in Unit I, ranging from ~2% to 20%. Authigenic P makes up a greater fraction of total P with increasing depth and age, with >80% in Unit II compared with ~60%–80% in Unit I.

Detrital P concentrations, which are not a component of reactive P, are greatest in Unit I (Fig. F1; Table T2), consistent with Site 1237 moving closer to the South American continent and increased volcanic activity in the Andes. Increases in detrital P are not necessarily coupled with increases in detrital barite. If there is an increase in detrital barite, our Ba/Ti ratio in the Ba_{excess} calculations should correct for this.

Although it is difficult to confirm that mass balance is maintained during the transformations from organic and oxide-associated P into authigenic P, we can compare the interstitial water P profile to a calculated "communication length for diffusion" (Gieskes, 1981). This is defined as the depth at which sediments are in diffusive communication with the overlying water column, z_c (meters), which is related by the porosity-corrected diffusion coefficient in sediments, pD_b, divided by the sedimentation rate, u (cm/1000 yr). Site 1237 has linear sedimentation rates ranging from 6.2 to 25.3 mcd/m.y. (Mix, Tiedemann, Blum, et

F5. $P_{reactive}$ and Ba_{excess} concentrations vs. depth, p. 16.
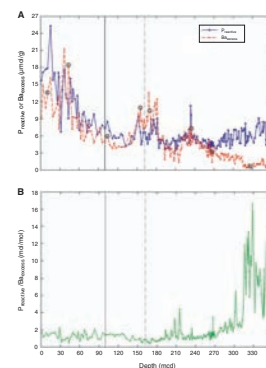
al., 2003). The communication length for P diffusion, calculated using these two extreme sedimentation rates and a diffusion coefficient of 2×10^{-6} cm^2/s (McDuff, 1978), is between ~250 and ~10,200 m. However, below the depth of maximum P concentration in the interstitial waters, authigenic P mineralization works to prevent P release into the overlying water column. The maximum interstitial water P concentration, 8.9 µM, is achieved at 6.37 mcd (Mix, Tiedemann, Blum, et al., 2003). Therefore, P release to the overlying water column is limited to the upper ~6 m of our record.

The redox state at the time of sediment burial is also of major concern, not only for P remobilization, but also for Ba$_{excess}$ and Ba$_{barite}$. Under sulfate-reducing conditions (SO$_4^{2-}$ < 20 mM), Ba can be remobilized, leading to barite loss (e.g., Faul et al., 2003). The majority of our U$_{EFs}$ are above crustal values, suggesting potentially reducing depositional environments. In sediments below the color contact boundary (~162 mcd), U$_{EFs}$ indicate less reducing conditions compared to the upper portion of Unit II and all of Unit I (Fig. F3A). However, authigenic U formation is not only influenced by changing redox conditions, it can be related to changes in productivity and organic carbon burial (Rosenthal et al., 1995; Chase et al., 2001; McManus et al., 2005). Therefore, above the color contact boundary and through Unit I, where we measure U$_{EFs}$ between ~3 and 13, this could be related to increases in carbon export and burial in these sediments, associated with possibly more reducing conditions.

Mn$_{EFs}$ are above the crustal average in all of Unit II and from the base of Unit I to ~50 mcd, suggesting oxygenated conditions in this portion of our record (Fig. F3B). Where we measured Mn$_{EFs}$ < 1, above 50 mcd in Unit I, this indicates less oxygenated conditions. The sharp decrease in Mn$_{EFs}$ coincides with the color contact boundary at ~162 mcd (Mix, Tiedemann, Blum, et al., 2003). The sudden decrease in Mn$_{EFs}$ and the observed sharp color change from pale brown (below 162 mcd) to grayish white (above 162 mcd) suggest that a change of paleoredox conditions from more oxygenated to slightly reducing burial of sediments are driving this event.

Another proxy related to carbon export and burial in sediments is biogenic barite. The comparison of two analytical methods of measuring biogenic barite, Ba$_{excess}$ and Ba$_{barite}$, found that in these samples Ba$_{excess}$ calculations resulted in higher estimates of biogenic Ba than did Ba$_{barite}$ extractions (Fig. F4; Table T3). We demonstrated that changing our Ba/Ti ratio used in the normalization calculations for Ba$_{excess}$ with published Ba/Ti ratios of varying source material does not dramatically change the comparison between the two methods of biogenic Ba measurements. In fact, for our samples compared here, there is no single Ba/Ti correction that will allow all of our Ba$_{excess}$ concentrations to be equal to the Ba$_{barite}$ estimates. Furthermore, these correction ratios are not within the range of Ba/Ti ratios found in common source materials.

Eagle et al. (2003) did a more extensive comparison between Ba$_{excess}$ and Ba$_{barite}$ using sediment core-top samples and varying the detrital component correction ratios (in their case using Ba/Al) for detrital Ba. The range of our data, ~0–11 µmol Ba/g in Ba$_{barite}$ and ~0–22 µmol Ba/g in Ba$_{excess}$, is within their range of published concentrations, ~0–19 in Ba$_{barite}$ and ~0–25 in Ba$_{excess}$. They found that calculating Ba$_{excess}$ values with different Ba/Al correction ratios resulted in Ba$_{excess}$ consistently greater than Ba$_{barite}$ and that there was no single Ba/Al ratio that would

result in Ba_{excess} and Ba_{barite} agreeing, and our results are consistent with these observations. Averyt and Paytan (2004) extended these results to comparisons of the calculated carbon export, molar ratios, and accumulation rates and found conflicting results among their biogenic barite proxies using the same core-top samples.

There are cautions in assuming that Ba_{barite} from sequential extractions is the absolute tracer for biogenic barite. Because our comparison (and that of Eagle et al., 2003), using different source materials to correct for detrital barite does not dramatically change the relationship between Ba_{barite} and Ba_{excess}, we believe there could be potential loss of biogenic barite during the sequential extraction procedure, thus accounting for consistently lower Ba_{barite} measurements. The two methods of measuring biogenic barite show that on long timescales (millions of years), the general trends in biogenic barite concentration are reflected in both, but the absolute values do not agree. This finding is similar to what other authors have found on shorter timescales (thousands of years) (Eagle et al., 2003; Averyt and Paytan, 2004). This implies that any quantitative conversions to carbon export should be made with caution, while understanding the assumptions made when interpreting each proxy. Future work should continue to explore this proxy comparison. Ideally, it would be best to measure biogenic barite by both methods to confirm the presence of barite crystals (Ba_{barite}) and measure the range of total barium (Ba_{excess}) that may be overlooked in the extraction procedure.

To determine if Site 1237 became more biologically productive throughout Unit I, we need to calculate accumulation rates of $P_{reactive}$ and Ba_{excess}. Some authors have shown that determining concentrations on a $CaCO_3$-free basis provides an estimate of trends in mass accumulation rates by accounting for $CaCO_3$ dilution (e.g., Averyt and Paytan, 2004; Faul and Paytan, 2005). This would work at Site 1237 in Unit II (predominantly composed of $CaCO_3$-rich sediments), but not in Unit I (predominantly siliceous sediments, also $CaCO_3$ and detrital material). Therefore, we do not make these calculations and present all our results in either concentration or molar ratios. This does not allow us to make firm conclusions about nutrient burial and carbon export and will require accumulation rate records.

If we use our redox-sensitive trace metal observations, interstitial water geochemistry, and the presence of pristine marine barite crystals to infer that both $P_{reactive}$ and Ba_{excess} can be used as valid paleoproductivity proxies, we can then attempt to compare and contrast both records to decipher possible changes in relative nutrient burial to carbon export burial at the sediment-water interface. We observe $P_{reactive}/Ba_{excess}$ ratios similar to expected modern values (Atlantic and Pacific = 2–13, as predicted from Dymond et al., 1992; Anderson and Sarmiento, 1994; and François et al., 1995) from the base of our record to ~180 mcd. This may suggest higher nutrient burial and lower export production (or lower barite preservation). The upper 180 mcd of our record falls below the expected range for modern sediments, and we suggest that this portion of the record could imply higher export production relative to nutrient burial. Low nutrient burial could suggest preferential $P_{reactive}$ regeneration that could fuel higher export productivity. $P_{reactive}/Ba_{excess}$ results are in agreement with the paleobacktracking of Site 1237. This site was ~20° farther west relative to the present location during the late Oligocene (Mix, Tiedemann, Blum, et al., 2003), placing Site 1237 away from the productive upwelling centers of Peru, the modern condition,

and into the edges of the oligotrophic subtropical gyre where carbon export is low and nutrient burial in the sediments should be low. Then, as the site approaches the chlorophyll-rich waters off Peru, carbon export to the sediments increases.

CONCLUSIONS

Our work has been to investigate and validate the geochemical proxies recording nutrient burial and primary productivity at Site 1237, which has been influenced by major tectonic and climatic changes during the evolution of the South Pacific. Until we have a confident age model with accurate sedimentation rates to calculate mass accumulation rates across time, we cannot provide firm conclusions about nutrient burial and paleoproductivity at this site. Trace metal EFs for U suggest possible reducing conditions during sediment burial. However, Mn enrichment data do not support a reducing environment. The sharp color change observed at ~162 mcd that coincides with the dramatic increase in Mn_{EFs} suggests that this event reflects a paleoredox boundary which changes from oxygenated to slightly reducing after the color change. Comparisons on selected samples of two methods of measuring biogenic barite, Ba_{excess} and Ba_{barite}, indicate that Ba_{excess} concentrations are greater than biogenic barite from sequential extractions. Using different Ba/Ti corrections for detrital Ba does not dramatically change these results. Caution must be used when using either proxy. We have shown that concentrations of $P_{reactive}$ are low in Unit II and increase in Unit I. Our other productivity proxy, Ba_{excess}, also shows generally lower concentrations in Unit II and increasing concentrations in Unit I. $P_{reactive}/Ba_{excess}$ ratios below ~180 mcd suggest nutrient burial is higher relative to organic carbon export to the sediments (ratios = 2–16). Throughout the upper 180 mcd, organic carbon export to the sediments was higher and nutrient burial was relatively low (ratios < 2), based on lower $P_{reactive}/Ba_{excess}$ ratios.

ACKNOWLEDGMENTS

REFERENCES

Anderson, L.A., and Sarmiento, J.L., 1994. Redfield ratios of remineralization determined by nutrient data analysis. *Global Biogeochem. Cycles,* 8(1):65–80. **doi:10.1029/93GB03318**

Anderson, L.D., and Delaney, M.L., 2000. Sequential extraction and analysis of phosphorus in marine sediments: streamlining of the SEDEX procedure. *Limnol. Oceanogr.,* 45:509–515.

Anderson, L.D., Delaney, M.L., and Faul, K.L., 2001. Carbon to phosphorus ratios in sediments: implications for nutrient cycling. *Global Biogeochem. Cycles,* 15(1):65–80. **doi:10.1029/2000GB001270**

Averyt, K.B., and Paytan, A., 2004. A comparison of multiple proxies for export production in the equatorial Pacific. *Paleoceanography,* 19(4):PA4003. **doi:10.1029/2004PA001005**

Bishop, J.K.B., 1988. The barite-opal-organic carbon association in oceanic particulate matter. *Nature (London, U. K.),* 332(6162):341–343. **doi:10.1038/332341a0**

Calvert, S.E., and Pedersen, T.F., 1993. Geochemistry of recent oxic and anoxic marine sediments: implications for the geological record. *Mar. Geol.,* 113(1–2):67–88. **doi:10.1016/0025-3227(93)90150-T**

Chase, Z., Anderson, R.F., and Fleisher, M.Q., 2001. Evidence from authigenic uranium for increased productivity of the glacial subantarctic ocean. *Paleoceanography,* 16(5):468–478. **doi:10.1029/2000PA000542**

Dehairs, F., Chesselet, R., and Jedwab, J., 1980. Discrete suspended particles of barite and the barium cycle in the open ocean. *Earth Planet. Sci. Lett.,* 49:528–550.

Delaney, M.L., and Anderson, L.D., 1997. Phosphorus geochemistry in Ceara Rise sediments. *In* Shackleton, N.J., Curry, W.B., Richter, C., and Bralower, T.J. (Eds.), *Proc. ODP, Sci. Results,* 154: College Station, TX (Ocean Drilling Program), 475–482. **doi:10.2973/odp.proc.sr.154.124.1997**

Delaney, M.L., and Anderson, L.D., 2000. Data report: phosphorus concentrations and geochemistry in California margin sediments. *In* Lyle, M., Koizumi, I., Richter, C., and Moore, T.C. (Eds.), *Proc. ODP, Sci. Results,* 167: College Station, TX (Ocean Drilling Program), 195–202. **doi:10.2973/odp.proc.sr.167.227.2000**

Dymond, J., and Collier, R., 1996. Particulate barium fluxes and their relationships to biological productivity. *Deep-Sea Res., Part II,* 43(4–6):1283–1308. **doi:10.1016/0967-0645(96)00011-2**

Dymond, J., Suess, E., and Lyle, M., 1992. Barium in deep-sea sediment: a geochemical proxy for paleoproductivity. *Paleoceanography,* 7:163–181.

Eagle, M., Paytan, A., Arrigo, K.R., van Dijken, G., and Murray, R.W., 2003. A comparison between excess barium and barite as indicators of carbon export. *Paleoceanography,* 18(1):1021. **doi:10.1029/2002PA000793**

Faul, K.L., Anderson, L.D., and Delaney, M.L., 2003. Late Cretaceous and early Paleogene nutrient and paleoproductivity records from Blake Nose, western North Atlantic Ocean. *Paleoceanography,* 18(2):1042. **doi:10.1029/2001PA000722**

Faul, K.L., and Delaney, M.L., 2000. Data report: phosphorus concentrations and geochemistry in Blake Nose sediments from Leg 171B. *In* Kroon, D., Norris, R.D., and Klaus, A. (Eds.), *Proc. ODP, Sci. Results,* 171B: College Station, TX (Ocean Drilling Program), 1–10. **doi:10.2973/odp.proc.sr.171B.120.2000**

Faul, K.L., and Paytan, A., 2005. Phosphorus and barite concentrations and geochemistry in Site 1221 Paleocene/Eocene boundary sediments. *In* Wilson, P.A., Lyle, M., and Firth, J.V. (Eds.), *Proc. ODP, Sci. Results,* 199: College Station, TX (Ocean Drilling Program), 1–23. **doi:10.2973/odp.proc.sr.199.214.2005**

Filippelli, G.M., and Delaney, M.L., 1995. Phosphorus geochemistry and accumulation rates in the eastern equatorial Pacific Ocean: results from Leg 138. *In* Pisias, N.G., Mayer, L.A., Janecek, T.R., Palmer-Julson, A., and van Andel, T.H. (Eds.), *Proc. ODP, Sci. Results,* 138: College Station, TX (Ocean Drilling Program), 757–767.

Filippelli, G.M., and Delaney, M.L., 1996. Phosphorus geochemistry of equatorial Pacific sediments. *Geochim. Cosmochim. Acta,* 60(9):1479–1495. **doi:10.1016/0016-7037(96)00042-7**

François, R., Honjo, S., Manganini, S.J., and Ravizza, G.E., 1995. Biogenic barium fluxes to the deep sea: implications for paleoproductivity reconstruction. *Global Biogeochem. Cycles,* 9(2):289–304. **doi:10.1029/95GB00021**

Ganeshram, R.S., François, R., Commeau, J., and Brown-Leger, S.L., 2003. An experimental investigation of barite formation in seawater. *Geochim. Cosmochim. Acta,* 67(14):2599–2605. **doi:10.1016/S0016-7037(03)00164-9**

Gieskes, J.M., 1981. Deep-sea drilling interstitial water studies: implications for chemical alteration of the oceanic crust, Layers I and II. *In* Warme, J.E., Douglas, R.G., and Winterer, E.L. (Eds.), *The Deep Sea Drilling Project: A Decade of Progress.* Spec. Publ.—Soc. Econ. Paleontol. Mineral., 32:149–167.

McDuff, R.E., 1978. Conservation behavior of calcium and magnesium in interstitial waters of marine sediments: identification and interpretation [Ph.D. dissert.]. Univ. of California, San Diego.

McManus, J., Berelson, W.M., Klinkhammer, G.P., Hammond, D.E., and Holm, C., 2005. Authigenic uranium: relationship to oxygen penetration depth and organic carbon rain. *Geochim. Cosmochim. Acta,* 69(1):95–108. **doi:10.1016/j.gca.2004.06.023**

Mix, A.C., Tiedemann, R., Blum, P., et al., 2003. *Proc. ODP, Init. Repts.,* 202: College Station, TX (Ocean Drilling Program). **doi:10.2973/odp.proc.ir.202.2003**

Nilsen, E.B., Anderson, L.D., and Delaney, M.L., 2003. Paleoproductivity, nutrient burial, climate change and the carbon cycle in the western equatorial Atlantic across the Eocene/Oligocene boundary. *Paleoceanography,* 18(3):1057. **doi:10.1029/2002PA000804**

Paytan, A., and Kastner, M., 1996. Benthic Ba fluxes in the central equatorial Pacific, implications for the oceanic Ba cycle. *Earth Planet. Sci. Lett.,* 142(3–4):439–450. **doi:10.1016/0012-821X(96)00120-3**

Paytan, A., Kastner, M., and Chavez, F.P., 1996. Glacial to interglacial fluctuations in productivity in the equatorial Pacific as indicated by marine barite. *Science,* 274(5291):1355–1357. **doi:10.1126/science.274.5291.1355**

Rosenthal, Y., Boyle, E.A., Labeyrie, L., and Oppo, D., 1995. Glacial enrichments of authigenic Cd and U in subantarctic sediments: a climatic control on the elements' oceanic budget? *Paleoceanography,* 10(3):395–414. **doi:10.1029/95PA00310**

Rudnick, R.L., and Gao, S., 2004. Composition of the continental crust. *In* Rudnick, R. (Ed.), *Treatise on Geochemistry* (Vol. 3): *The Crust:* Amsterdam (Elsevier), 1–64.

Ruttenberg, K.C., 1992. Development of a sequential extraction method for different forms of phosphorus in marine sediments. *Limnol. Oceanogr.,* 37:1460–1482.

Ruttenberg, K.C., and Berner, R.A., 1993. Authigenic apatite formation and burial in sediments from non-upwelling, continental margin environments. *Geochim. Cosmochim. Acta,* 57(5):991–1007. **doi:10.1016/0016-7037(93)90035-U**

Turekian, K.K., and Wedepohl, K.H., 1961. Distribution of the elements in some major units of the Earth's crust. *Geol. Soc. Am. Bull.,* 72:175–192.

Tyrrell, T., 1999. The relative influences of nitrogen and phosphorus on oceanic primary production. *Nature (London, U. K.),* 400(6744):525–531. **doi:10.1038/22941**

Figure F1. Operationally defined components of total phosphorus vs. depth: oxide-associated, authigenic, organic, and detrital P. Solid vertical line at 100 mcd divides the two main lithologic units described on board the ship, Unit I (<100 mcd) and Unit II (>100 mcd). The sediment color changes abruptly at ~162 mcd, dashed vertical line, from a fairly homogeneous pale brown (below 162 mcd) to grayish white (above 162 mcd) (Mix, Tiedemann, Blum, et al., 2003).
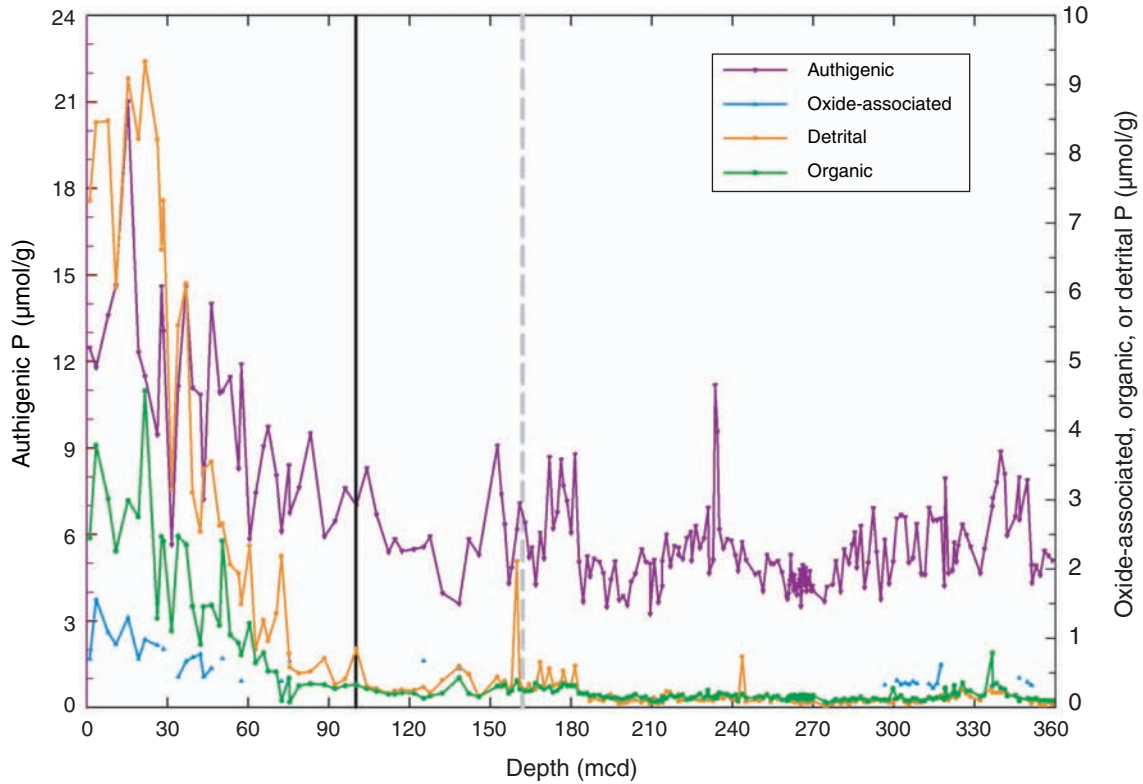
Figure F2. Al and Ti crossplot. Dashed regression line is $y = 38.7x + 28.6$, $R^2 = 0.97$, $n = 220$.
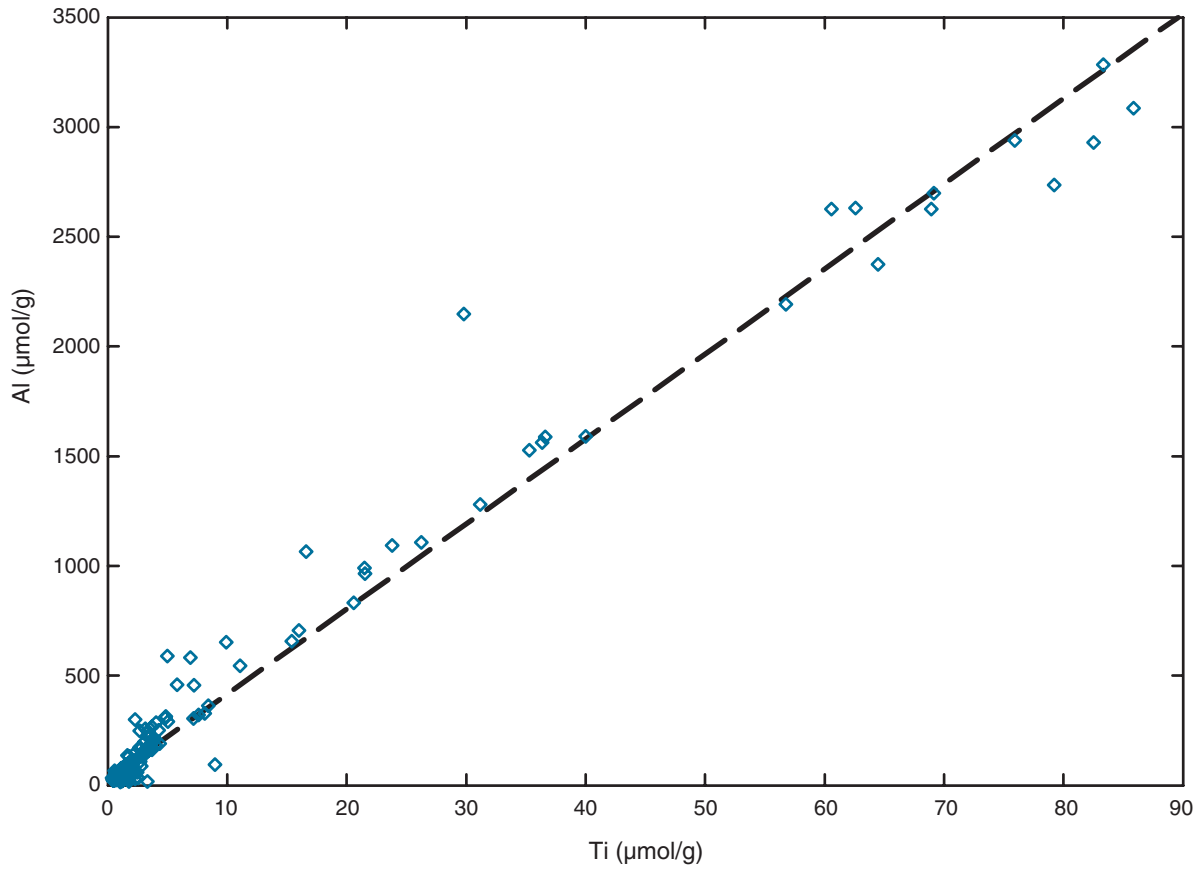
Figure F3. A. U enrichment factors (U_{EFs}) calculated from measured U concentrations and using the crustal U/Ti of 0.142 mmol/mol (Rudnick and Gao, 2004) vs. depth. **B.** Mn enrichment factors (Mn_{EFs}) calculated from measured Mn concentrations and using the crustal molar Mn/Ti of 0.176 (Rudnick and Gao, 2004) vs. depth. Solid horizontal line is EF = 1 (no enrichment or depletion relative to presumed crustal source). Solid vertical line at 100 mcd divides the two main lithologic units described on board the ship, Unit I (<100 mcd) and Unit II (>100 mcd). Dashed vertical line at 162 mcd is depth of observed color contact boundary.
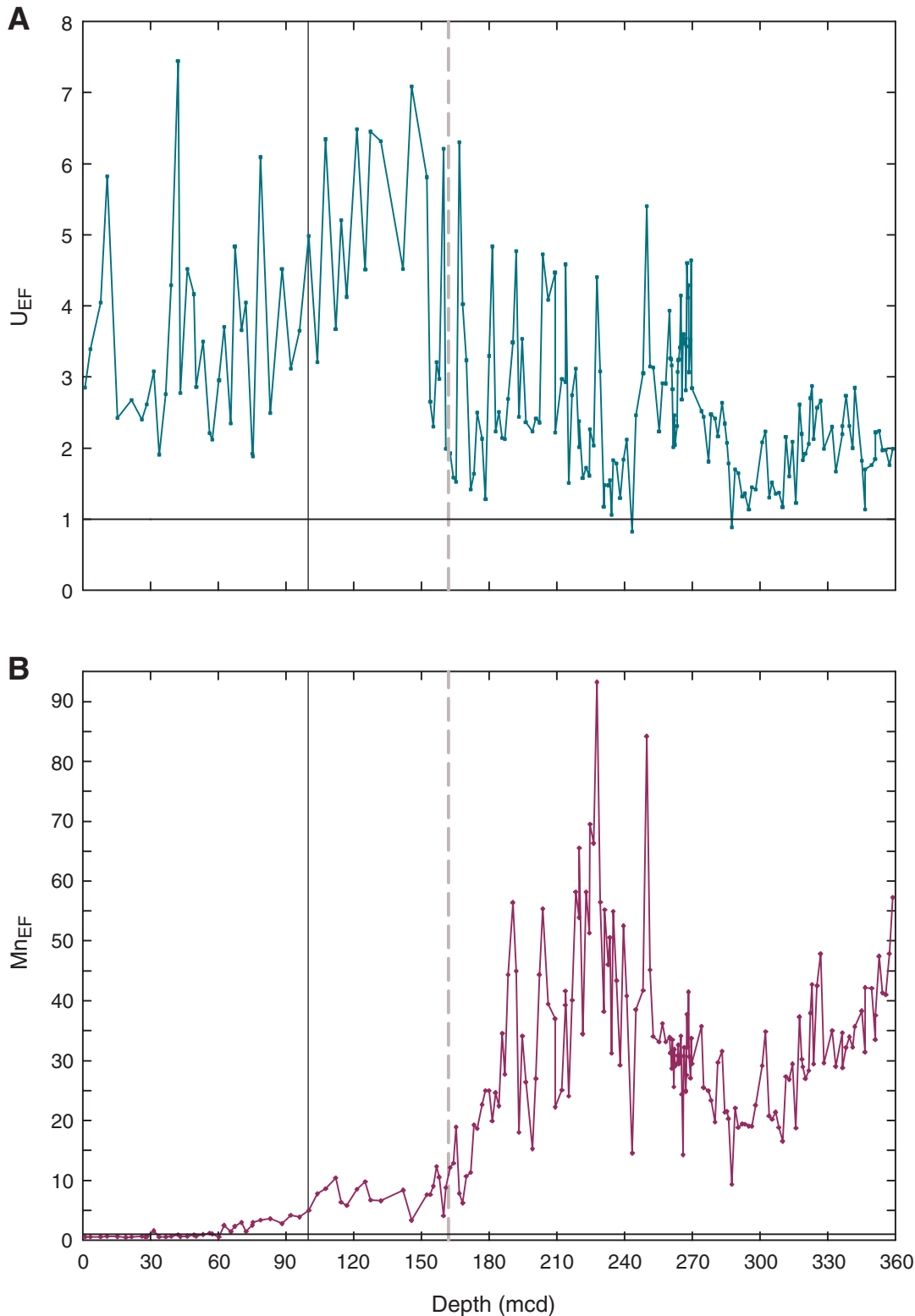
Figure F4. Comparison of Ba_{excess} and Ba_{barite}, Ba in biogenic barite as determined by total acid digestion (Ba_{excess}) using the molar Ba/Ti = 0.009 for carbonates (Turekian and Wedepohl, 1961), Ba/Ti = 0.037 for bulk crustal (Rudnick and Gao, 2004), Ba/Ti = 0.043 for Ca-rich granites (Turekian and Wedepohl, 1961), Ba/Ti = 0.057 for the upper crust (Rudnick and Gao, 2004), and Ba/Ti = 0.174 for deep-sea clays (Turekian and Wedepohl, 1961) for selected samples vs. Ba in biogenic barite determined by sequential extraction (Ba_{barite}). Solid line is linear regression for upper crust values: $y = 1.24x + 3.91$, $R^2 = 0.79$, $n = 8$. Dashed line is 1:1. See also data in Table T3, p. 19.
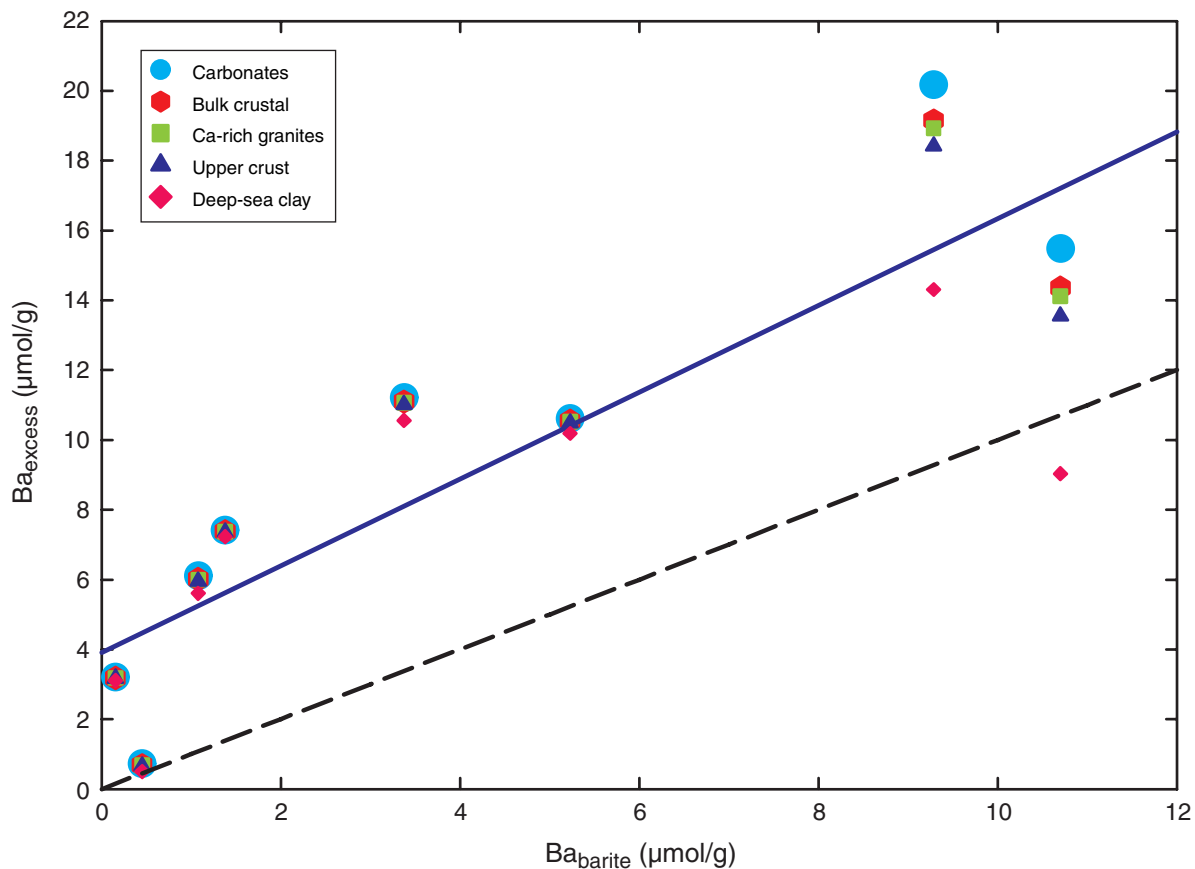
Figure F5. A. $P_{reactive}$ and Ba_{excess} concentrations vs. depth. $P_{reactive}$ (µmol P/g) is the sum of oxide-associated, authigenic, and organic P; Ba_{excess} (µmol Ba/g), is defined as total Ba corrected for detrital inputs using the molar Ba/Ti upper crustal ratio of 0.057 (Rudnick and Gao, 2004) and measured Ti concentrations. Black circles indicate samples that were used for the Ba_{barite} comparison (see Fig. F4, p. 15). **B.** $P_{reactive}/Ba_{excess}$ ratio vs. depth. Solid vertical line at 100 mcd divides the two main lithologic units described on board the ship, Unit I (<100 mcd) and Unit II (>100 mcd). Dashed vertical line at 162 mcd is depth of observed color contact boundary.
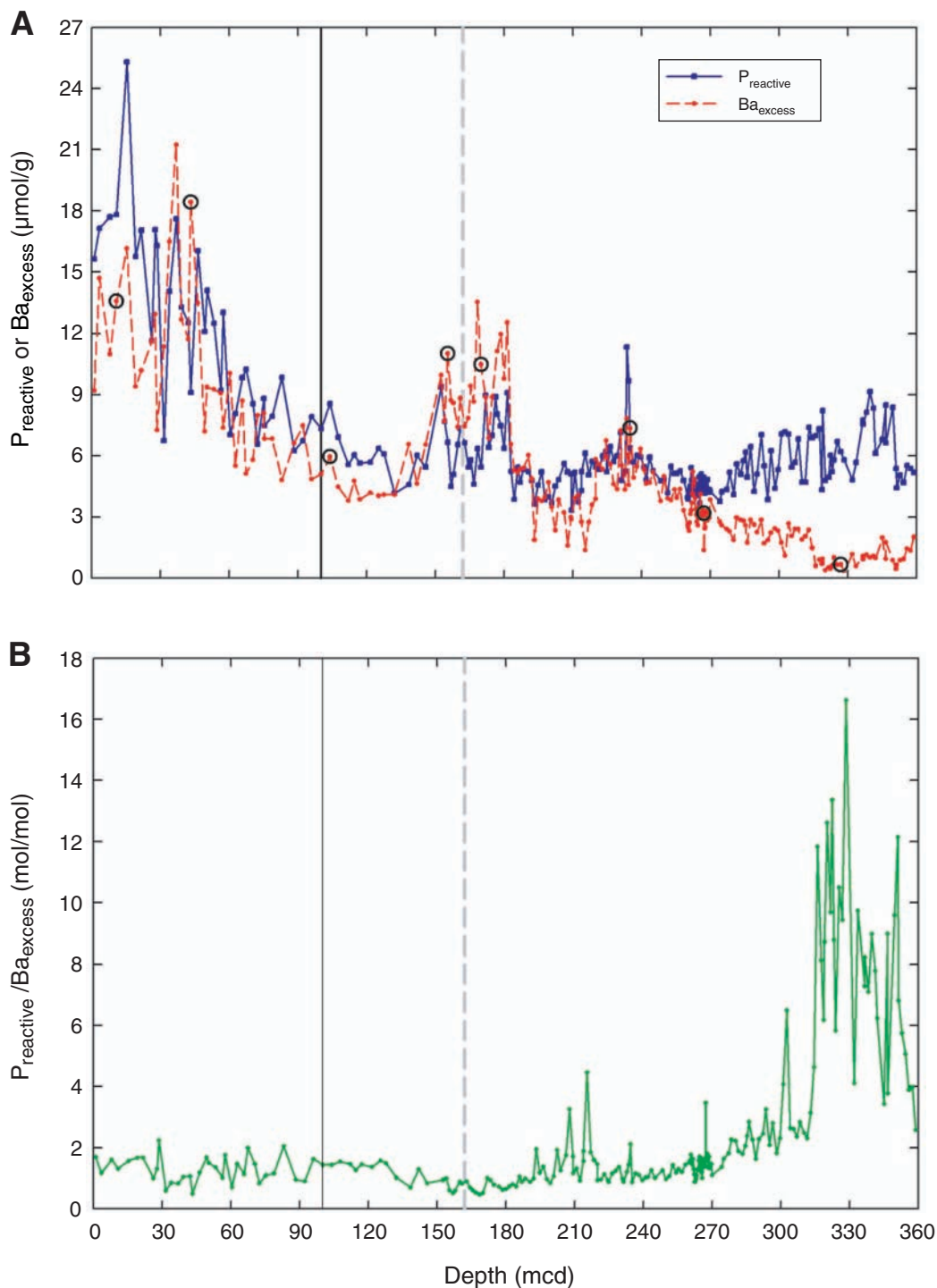
Table T1. Analytical figures of merit.

| | Phosphorus concentration (µmol P/g sediment) | | | | Trace metal concentration (µmol/g sediment) | | | | |
	Oxide-associated	Authigenic	Organic	Detrital	Al	Ti	Mn	U*	Ba
Detection limits[†]	0.27	0.17	0.02	0.01	0.01	0.49	0.02	0.04	0.12
Consistency standard[‡]	BDL	5.95 ± 0.76	0.21 ± 0.03	0.28 ± 0.09	159 ± 17.1	2.71 ± 0.33	6.61 ± 0.57	1.29 ± 0.07	6.23 ± 0.91

Notes: * = nmol/g sediment. † = defined as three times the standard deviation of replicate measures of a blank (which is of the same matrix as each extractant or digestion) and expressed in equivalent concentration for a sediment sample; Al and Ba were measured on the ICP-OES; Ti, Mn, and U were measured on the ICP-MS. ‡ = consistency standard is composed of a homogenized mixture of Site 1237 samples and was included in each run to evaluate between-run analytical reproducibility. BDL = below detection limit.

Table T2. Concentrations of phosphorus components and trace metals from Leg 202, Site 1237 sediments. (This table is available in an **oversized format.**)

Table T3. Ba_{barite} and Ba_{excess} comparison.

Core, section, interval (cm)	Depth (mbsf)	Depth (mcd)	CaCO$_3$ (wt%)	(µmol/g sediment)			Ba_{excess} (µmol/g sediment)*				
				Ba[†]	Ti[†]	Ba_{barite}[‡]	Carbonates Ba/Ti = 0.009**	Bulk crustal Ba/Ti = 0.037[††]	Ca-rich granites Ba/Ti = 0.043**	Upper crust Ba/Ti = 0.057[††]	Deep-sea clay Ba/Ti = 0.174**
202-1237C-											
2H-2, 113–115	11.94	10.84	37.0	15.8	40.0	10.7	15.5	14.4	14.1	13.6	9.0
5H-2, 113–115	40.44	43.31	59.0	20.5	36.3	9.28	20.2	19.2	18.9	18.4	14.3
202-1237D-											
7H-5, 17–19	96.00	104.02	91.1	6.13	3.07	1.08	6.10	6.02	6.00	5.96	5.61
202-1237B-											
16H-3, 113–115	142.64	155.34	86.8	11.2	4.06	3.38	11.2	11.1	11.1	11.0	10.6
17H-5, 113–115	155.16	169.96	88.3	10.6	2.67	5.23	10.6	10.5	10.5	10.5	10.2
202-1237C-											
23H-2, 113–115	213.44	235.04	94.2	7.43	1.16	1.38	7.42	7.38	7.38	7.36	7.23
202-1237D-											
10H-6, 46–48	242.01	266.91	95.6	3.21	0.57	0.16	3.20	3.19	3.18	3.17	3.11
202-1237C-											
31H-4, 73–75	292.07	326.93	94.9	0.74	1.37	0.45	0.72	0.69	0.68	0.66	0.50

Notes: * = Ba_{excess} = Ba_{total} – [Ti * Ba/Ti$_{source}$ material]. † = total sediment digestion. ‡ = barite extraction. ** = Turekian and Wedepohl (1961). †† = Rudnick and Gao (2004).